1 ρ resonance model

New scalar and vector particles with enhanced couplings to W, Z bosons and/or to the top quark are predicted by many models, e.g. the Standard Model heavy Higgs boson, Z' bosons or the new strong vector resonance from the Strong Electroweak Symmetry Breaking (SESB). Here we consider the last alternative, a minimal model for a triplet of new strong vector particles, ρ ($\rho^{\pm}, \rho^0$), based on the BESS model [1] of the SESB.

It is minimal in the sense that ρ is the only new particle added to the spectrum of the Standard Model (SM). It effectively replaces the SM Higgs boson, keeping the relevant symmetries of the Higgs sector: $SU(2)_L \times U(1)_Y$ local and $SU(2)_L \times SU(2)_R$ global (there are violations of the latter equivalent to those in the SM). The model is described by the effective chiral Lagrangian with the details given in [2].

We will concentrate here on the interactions of the neutral ρ^0 with the longitudinal W (ρ^0 does not couple directly to the longitudinal Z) and with the top quark. They can be described by the following simple Lagrangian to which the relevant parts of the original chiral efective Lagrangian can be reduced :

$$\begin{aligned}
\mathcal{L}_{\rho\pi\pi} &= +ig_\pi \frac{M_\rho}{v}(\pi^- \partial^\mu \pi^+ - \pi^+ \partial^\mu \pi^-)\rho^0_\mu \\
\mathcal{L}_{\rho tt} &= g_1^t \bar{t}\gamma^\mu t\ \rho^0_\mu + g_2^t \bar{t}\gamma^\mu \gamma^5 t\ \rho^0_\mu;
\end{aligned}$$

where π represent longitudinal W bosons and the coupling constants g_π, g_1^t (we assume $g_1^t = g_2^t$) can be expressed in terms of the coupling constants of the effective chiral Lagrangian g'', b_2 as : $g_\pi = M_\rho/(2\ vg'') + \mathcal{O}(g^2/g''^2)$, $g_1^t = g'' b_2/4 + \mathcal{O}(g^2/g''^2)$. The limits from low energy experiments give $g'' \gtrsim 10$, $|b_2| \lesssim 0.08$.

The width of ρ^0 is defined by its mass and couplings g'', b_2. We show the partial width $\Gamma(\rho \to W^+W^-)$ and the total width Γ in Figs. 1a,b,c,d as function of $g'' \equiv g_v$ and b_2 for three different masses of ρ^0 (700, 1500, 3000 GeV).

We define the 'No-resonance model' as the limit $M_\rho \to \infty, g'' \to \infty, b_2 \to 0$ of our ρ model. It is effectively identical with the Higgsless Standard Model. We use this model to find the continuum (irreducible) background in our studies.

2 LHC processes introduction

At LHC, a natural process for ρ resonance studies is $WW \to \rho \to WW$ fusion ($pp \to jjWW + X$) and $WW \to \rho \to t\bar{t}$ fusion ($pp \to jjt\bar{t} + X$). While the $WW \to WW$ process (which depends on g_π) was found sensitive to the ρ presence by many studies (just like heavy Higgs in the same channel), the $WW \to t\bar{t}$ (which depends on the product $g_\pi g_1^t$) was found to be completely swamped by the huge QCD $t\bar{t}$ background. There are, however, other processes potentially sensitive to the ρ resonance: $pp \to \rho t\bar{t}$ with ρ subsequently decaying to either a W^+W^- pair (proportional to the $g_\pi g_1^t$ product) or $t\bar{t}$ pair (proportional to $(g_1^t)^2$). Below we discuss our first results obtained with CompHEP package.

3 $pp \to \rho t\bar{t}$ analysis

This is fast analysis with 3 particles in the final state. The cross sections for $pp \to W^+W^-t\bar{t}, t\bar{t}t\bar{t}$ are found from the cross sections for $pp \to \rho t\bar{t}$, multiplied by the corresponding branching ratios (branching ratio approximation, BRA).

The dominant gluon-gluon (gg) channel consists of 8 diagrams (Fig.2). $q\bar{q}$ channels were neglected.

The total cross section is plotted as a function of b_2 and $g'' \equiv g_v$ in Figs. 3a,4a,5a for $M_\rho = 700, 1500, 3000$ GeV in the context of $pp \to W^+W^-t\bar{t}$ results and again in Figs. 10a, 11a in the context of $pp \to t\bar{t}t\bar{t}$ results. We imposed cuts on the transverse momentum and rapidity of both top quarks:

$$\begin{aligned} p_T(t), p_T(\bar{t}) &> 100 \text{ GeV}, \\ -2 < Y(t), Y(\bar{t}) &< 2. \end{aligned} \tag{1}$$

We show branching ratios for $\rho \to t\bar{t}$ in Figs. 3b,4b,5b (and again in Figs. 10b, 11b). Branching ratio for $\rho \to W^+W^-$, $\mathrm{BR}(WW) = 1 - \mathrm{BR}(t\bar{t})$.

The cross section for $pp \to \rho t\bar{t} \to W^+W^-t\bar{t}$ was calculated as $\sigma(W^+W^-t\bar{t}) = \sigma(pp \to \rho t\bar{t}) \times BR(WW)$ and plotted in Figs. 3c,4c,5c.

Finally, the cross section for $pp \to \rho t\bar{t} \to t\bar{t}t\bar{t}$ was calculated as $\sigma(t\bar{t}t\bar{t}) = \sigma(pp \to \rho t\bar{t}) \times BR(t\bar{t})$ and plotted in Figs. 10c, 11c.

4 $pp \to W^+W^-t\bar{t}$ analysis

This is more involved analysis with 4 particles in the final state with W^+, W^- not necessarily coming from the ρ resonance. The motivation is to go beyond the BRA of the previous section. Currently we use this approach mainly for the continuum irreducible background computation. The signal *multiparameter* computation will follow sometime later.

There are 39 diagrams in the dominant gg channel (some of them are shown in Fig. 5e) and 131 diagrams in the $u\bar{u}$ channel. We normally neglect $q\bar{q}$ channels, the only exception is the illustrative number for the background given below (0.013 fb).

As illustration we choose ρ with $M_\rho = 700$ GeV, $b_2 = 0.08, g'' = 10$ ($\Gamma_\rho = 3.95$ GeV). With no cuts, the total cross section is 10.2 fb and various distributions are plotted in Figs. 6,7,8. With cuts defined as

$$\begin{aligned} 700 - 3\Gamma_\rho < M_{WW} < 700 + 3\Gamma_\rho \ \ (\text{GeV}) \\ p_T(t), p_T(\bar{t}) > 100 \text{ GeV} \\ -2 < Y(t), Y(\bar{t}) < 2, \end{aligned} \tag{2}$$

the cross section is 0.96 fb. This is to be compared with the BRA calculation of the previous section which gives $\sigma(W^+W^-t\bar{t}) = \sigma(pp \to \rho t\bar{t}) \times BR(WW) = 4.35 fb \times 0.24 = 1.04 fb$.

The irreducible continuum background [1] with the cuts of Eq.2 is 0.037 fb for the gg channel and 0.013 fb for the $u\bar{u}$ channel.

4.1 Statistical significance for $pp \to W^+W^-t\bar{t}$

To calculate statistical significance R we used BRA cross sections for the signal, $\sigma(W^+W^-t\bar{t}) = \sigma(pp \to \rho t\bar{t}) \times BR$, and we considered only the gg-channel for the irreducible background. We assume integrated luminosity $L = 100\ fb^{-1}$. For our illustrative 700 GeV resonance ($b_2 = 0.08, g'' = 10$, $\Gamma_\rho = 3.95$ GeV) we thus get $R = \frac{S}{\sqrt{B}} = \frac{104}{\sqrt{3.7}} \doteq 54$. R as a function of g_V and b_2 is plotted in Figs. 3d,4d,5d.

[1] Continuum on which the ρ peak sits. It is represented by the no-resonance model defined as heavy ρ limit of the ρ model: $M_\rho = 30000$ GeV, $b_2 = 0, g'' = 1000$.

5 $pp \to t\bar{t}t\bar{t}$ analysis

Again, the motivation is to go beyond the BRA. Currently we use this approach for the continuum irreducible background computation only. The signal computation will follow in the future.

We consider only the dominant gg-channel with 54 diagrams (uu channel, e.g., has 49 diagrams). Some of the diagrams are shown in Fig. 9. Following CompHEP, we assigned numbers 3 and 4 to the top quarks and numbers 5 and 6 to the antitop quarks and then imposed the following cuts (combination 35+46 is picked at random out of 4 possible $t\bar{t}$ pairings, the other three being 36+45,45+36,46+35)

$$\begin{gathered} M_\rho - 3\Gamma_\rho < M_{35} < M_\rho + 3\Gamma_\rho \;\; \text{(GeV)} \\ p_T(4), p_T(6) > 100 \text{ GeV} \\ -2 < Y(4), Y(6) < 2, \end{gathered} \tag{3}$$

These cuts suppress (underestimate) the true cross section by a factor of 4 for a narrow interval $(M_\rho - 3\Gamma_\rho, M_\rho + 3\Gamma_\rho)$ (the peak region). This is because the remaining three $t\bar{t}$ pairings each contribute the same amount in the peak region as does the 35+46 pairing, but do not survive the above cuts. For a large interval $(M_\rho - 3\Gamma_\rho, M_\rho + 3\Gamma_\rho)$, the suppression factor gradually decreases from 4 to 1.

5.1 Statistical significance for $pp \to t\bar{t}t\bar{t}$

Again, to calculate statistical significance we used BRA cross sections for the signal obtained as $\sigma(pp \to t\bar{t}t\bar{t}) = \sigma(pp \to \rho t\bar{t}) \times BR$ (Figs. 10c, 11c) . We compensate the suppression factor for the irreducible continuum background by multiplying the cross section by a factor of 4. As discussed above, this tends to overestimate the background for broad resonances (for which the suppression is smaller). We assume integrated luminosity $L = 100\ fb^{-1}$. R as a function of g_V and b_2 is plotted in Figs. 10d, 11d.

6 Discussion

We would like to point out a couple of points. For R calculations we used approximate calculations of the cross sections via BRA. This is a good approximation for *narrow* ρ only .

We assumed fixed width of ρ in the propagators.

We did not consider the issues of the W boson and the top quark decays and reconstruction efficiences which will significantly modify our predictions of the statistical significance R.

We chose the $p_T > 100$ GeV and Y cuts somewhat arbitratrily, not really understanding the experimental requirements.

Finally, the only background we considered is the No-resonance, irreducible continuum. We realize there might be reducible background processes as well.

As a next step we can compute $\sigma(W^+W^-t\bar{t}), \sigma(t\bar{t}t\bar{t})$ directly without BRA.

References

[1] R. Casalbuoni et al: *Phys. Lett.* **B155** (1985), p.95; D. Dominici: *Riv. Nuovo Cim.* **20** (1997), p.1; R. Casalbuoni et al: *Phys. Lett.* **B258**, (1991) p.161.

[2] M. Gintner, I. Melo: *Acta Phys. Slovaca* **51** (2001), p.139.

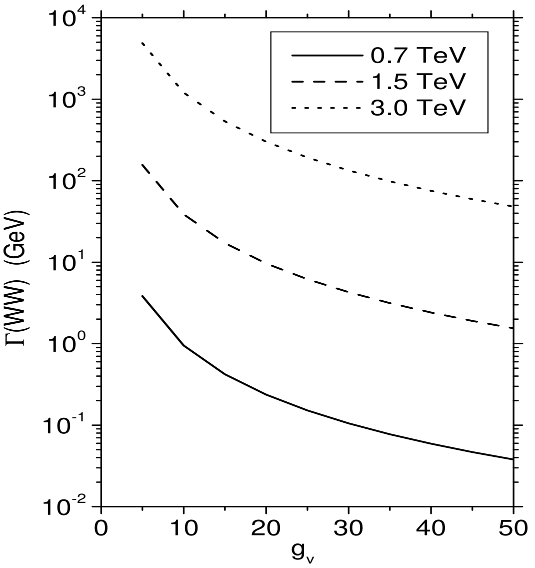

Fig.1a *Partial width* $\rho \to WW$

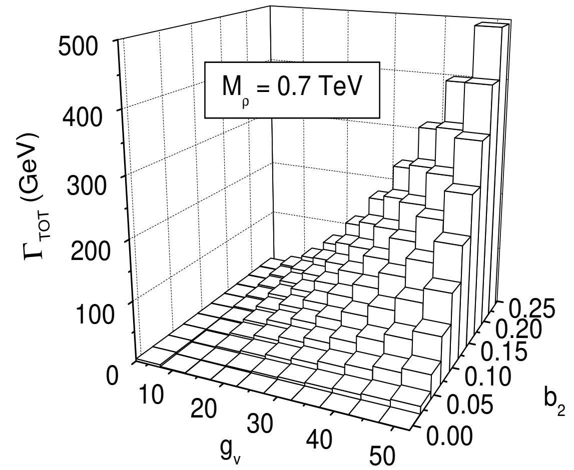

Fig. 1b *Total width* $\rho \to WW + t\bar{t}$

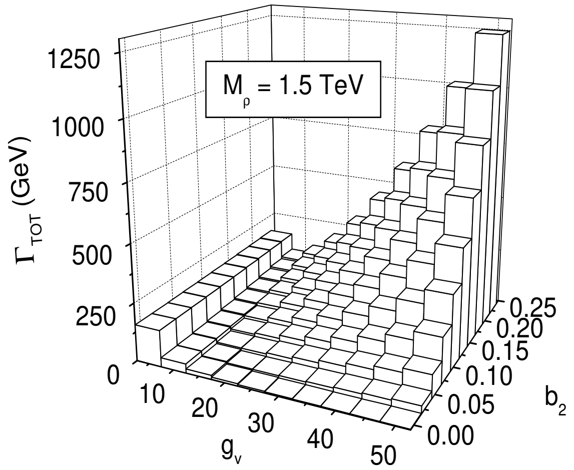

Fig.1c *Total width* $\rho \to WW + t\bar{t}$

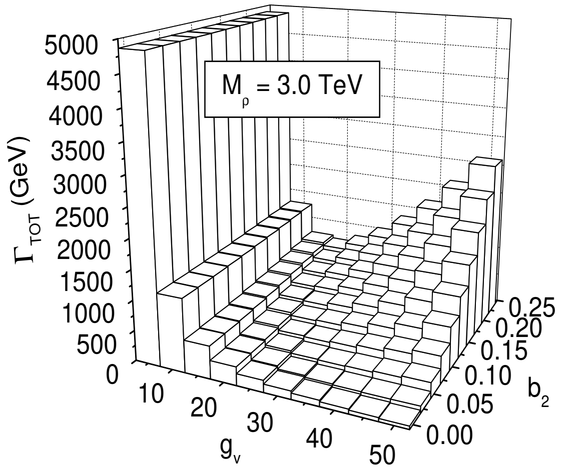

Fig.1d *Total width* $\rho \to WW + t\bar{t}$

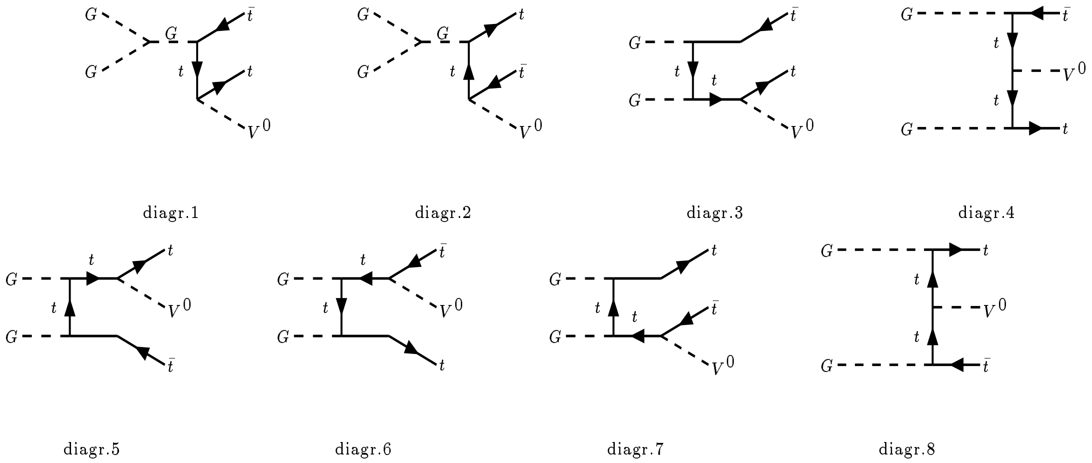

Fig.2 *The dominant gluon-gluon channel diagrams for* $pp \to \rho\, t\bar{t}$

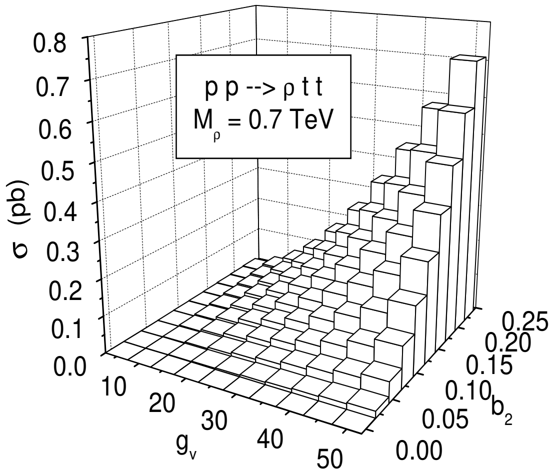

Fig.3a $\sigma(pp \to \rho t\bar{t})$

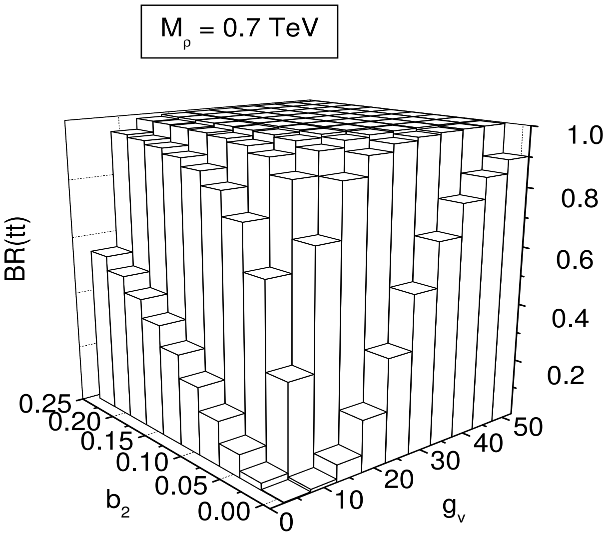

Fig.3b $BR(t\bar{t})$. $BR(WW)$ = *1*-$BR(t\bar{t})$

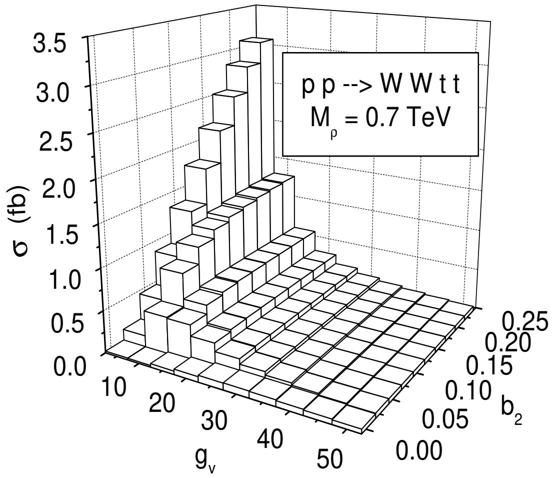

Fig.3c $\sigma = \sigma(pp \to \rho t\bar{t}) \times BR(WW)$

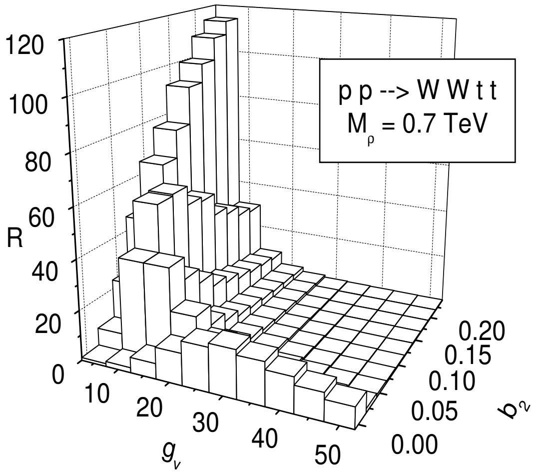

Fig.3d *Statistical significance R*

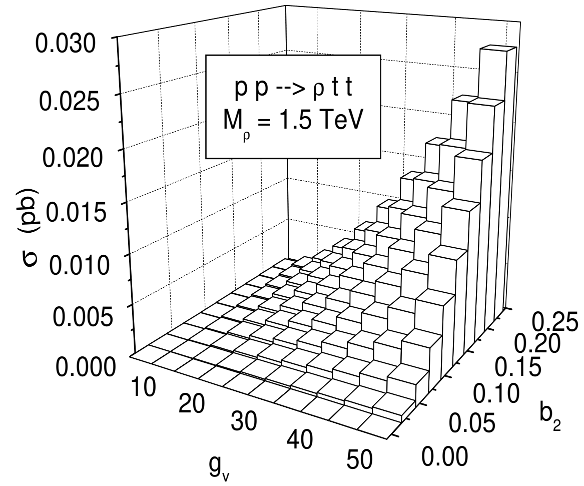

Fig.4a $\sigma(pp \to \rho t\bar{t})$

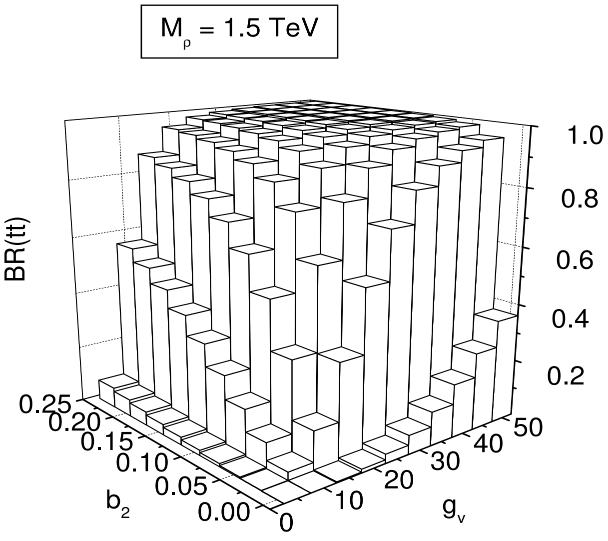

Fig.4b $BR(t\bar{t})$. $BR(WW)$ = 1-$BR(t\bar{t})$

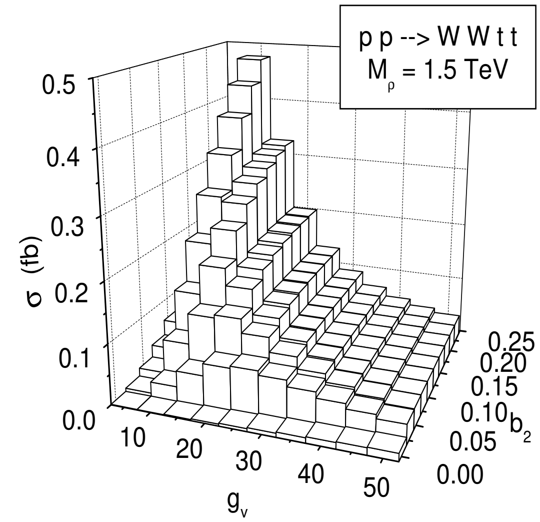

Fig.4c $\sigma = \sigma(pp \to \rho t\bar{t}) \times BR(WW)$

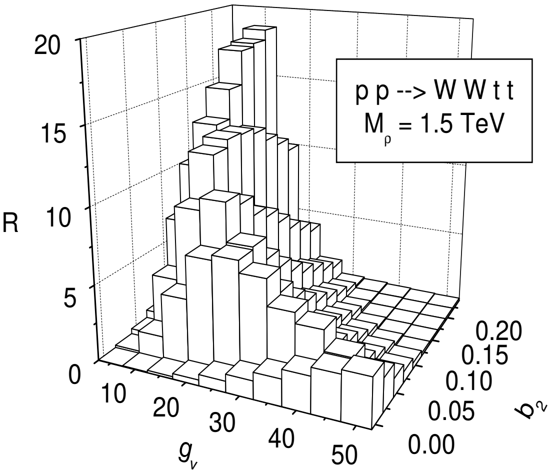

Fig.4d *Statistical significance R*

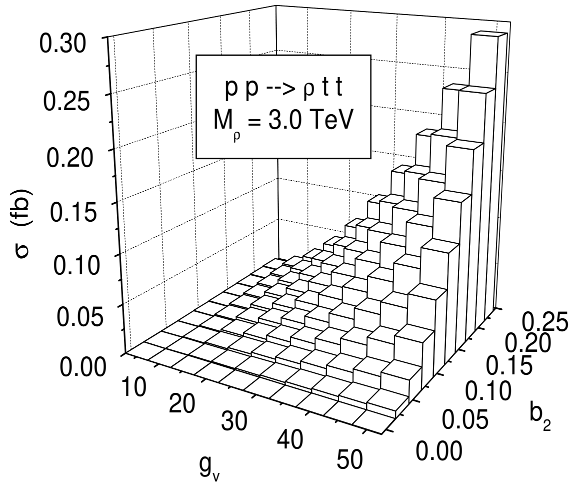

Fig.5a $\sigma(pp \to \rho t\bar{t})$

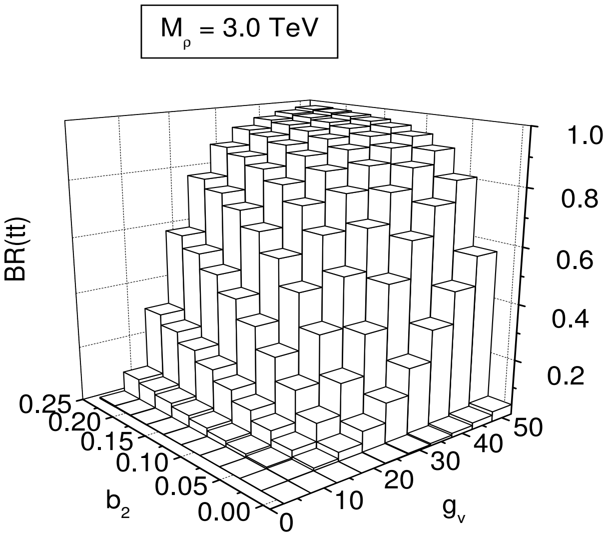

Fig.5b $BR(t\bar{t})$. $BR(WW)$ = 1-$BR(t\bar{t})$

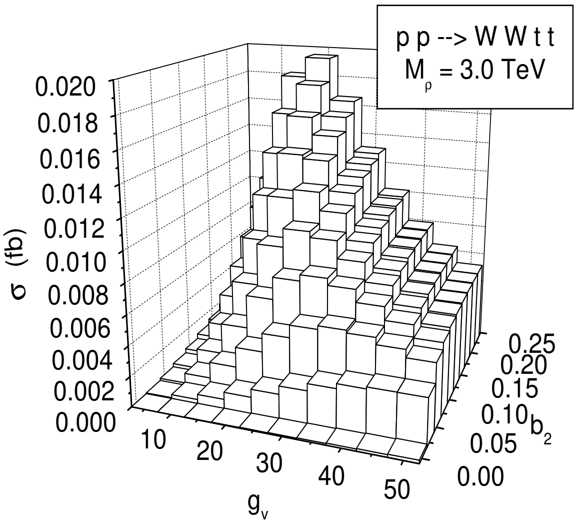

Fig.5c $\sigma = \sigma(pp \to \rho t\bar{t}) \times BR(WW)$

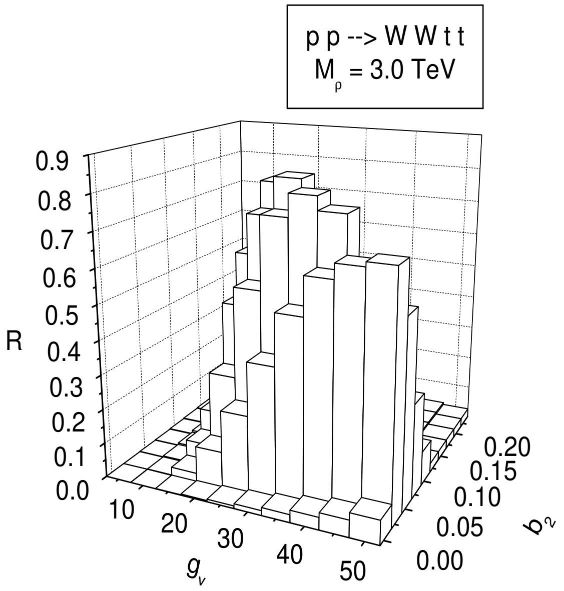

Fig.5d *Statistical significance* R

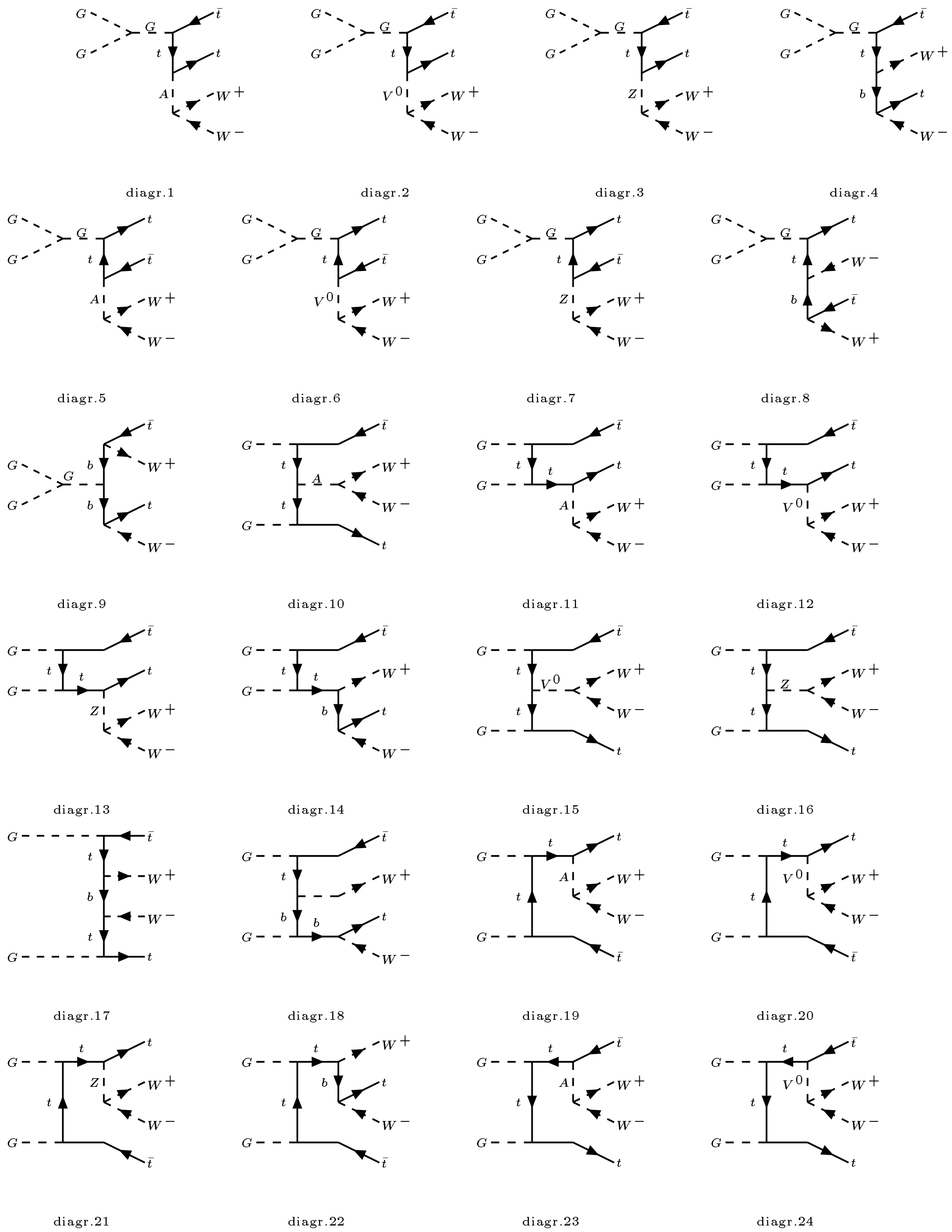

Fig.5e *Some of the dominant gluon-gluon channel diagrams for* $pp \to W^+W^-\ t\bar{t}$

Fig. 6 $pp \to gg \to W^+W^-t\bar{t}$: M_{WW} (top) and $t\bar{t}$ (bottom) distributions. $M_\rho = 0.7\ TeV$, $g_v = 10, b_2 = 0.08$, $\Gamma_\rho = 3.95$ GeV

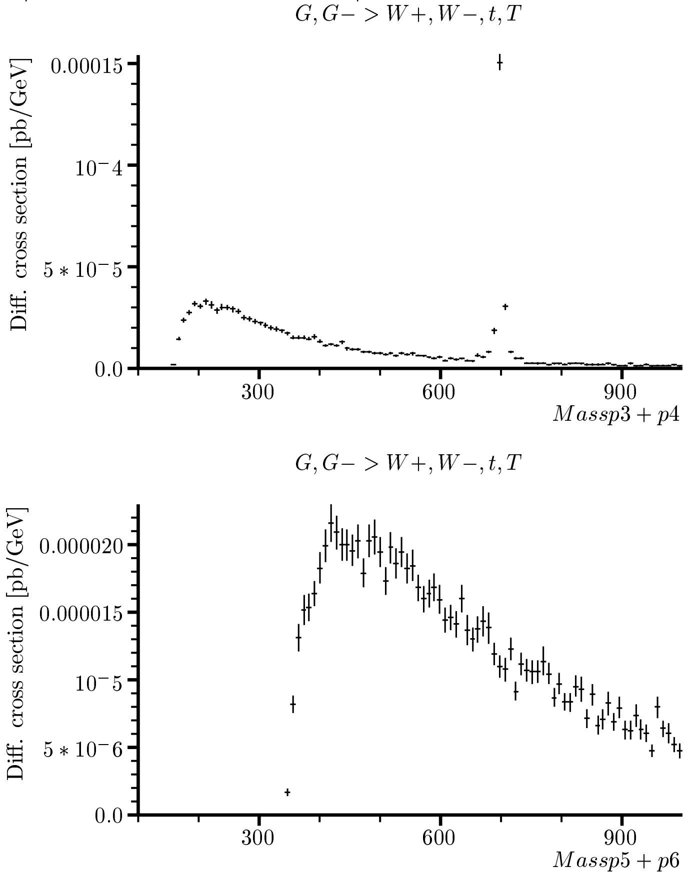

Fig. 7 $pp \to gg \to W^+W^-t\bar{t}$: distributions in $p_T(W^+)$ (top), $p_T(WW)$ (bottom left) and $p_T(t)$ (bottom right) .

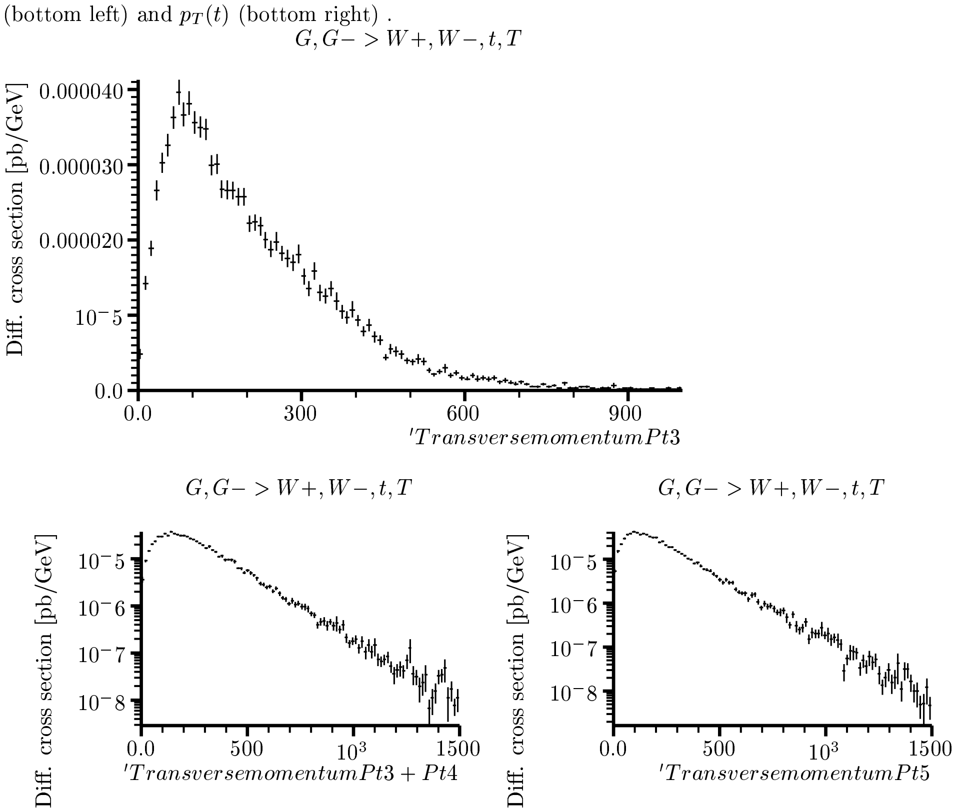

Fig. 8 $pp \to gg \to W^+W^-t\bar{t}$: distributions in $p_T(tt)$ (top left), $y(W^+)$ (top right), $y(W^-)$ (center left), $y(W^+W^-)$ (center right), $y(t)$ (bottom left) and $y(\bar{t})$ (bottom right) .

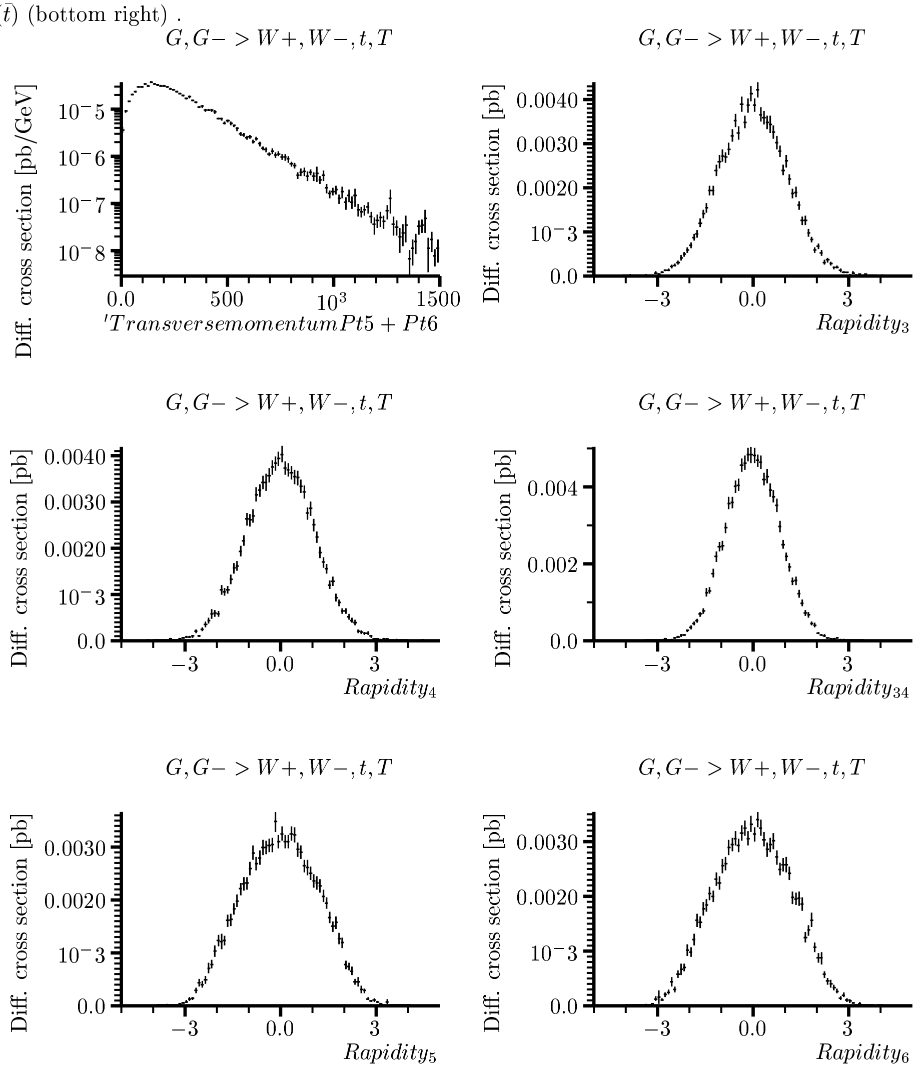

1

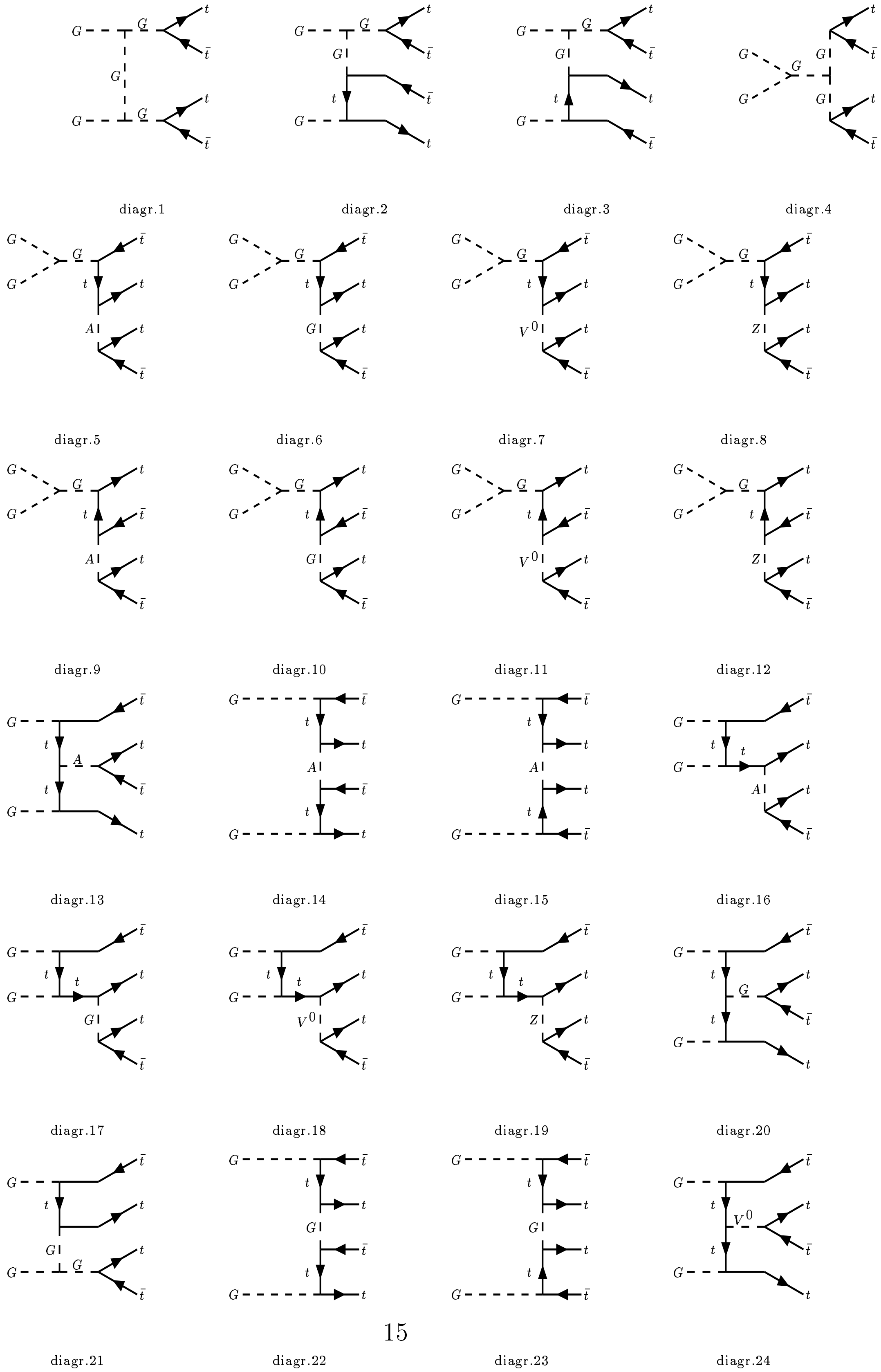

1

Fig.9 *Some of the dominant gluon-gluon channel diagrams for* $pp \to t\bar{t}\, t\bar{t}$

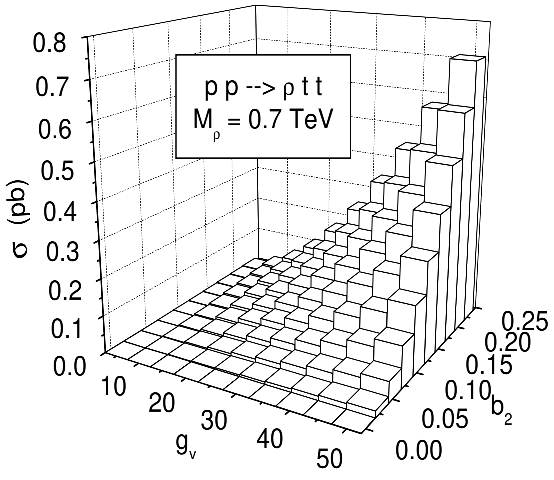

Fig.10a $\sigma(pp \to \rho t\bar{t})$

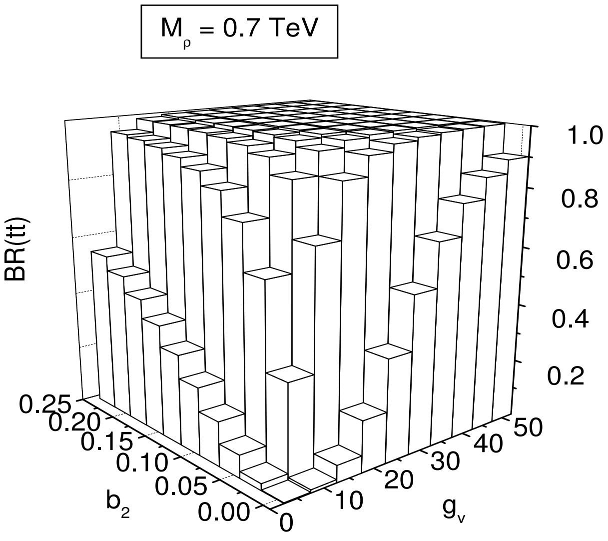

Fig.10b $BR(t\bar{t})$

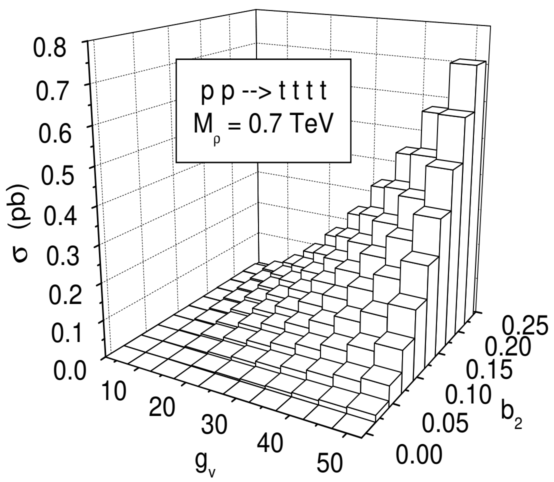

Fig.10c $\sigma = \sigma(pp \to \rho t\bar{t}) \times BR(t\bar{t})$

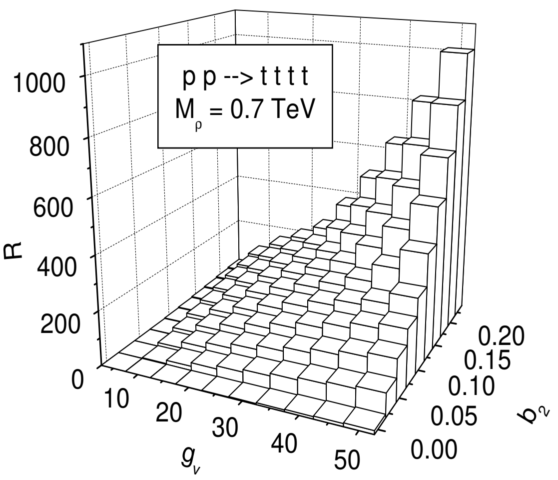

Fig.10d *Statistical significance R*

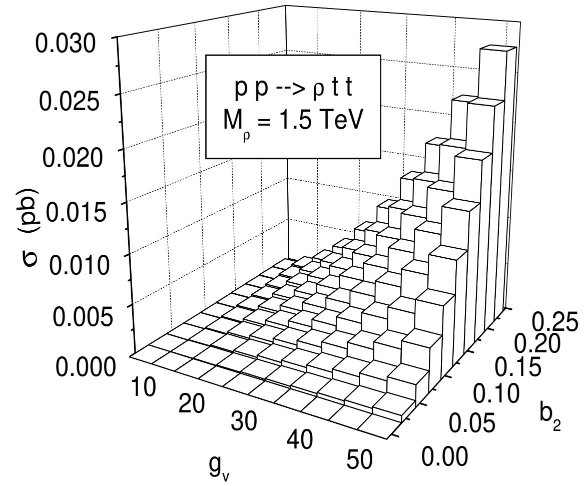

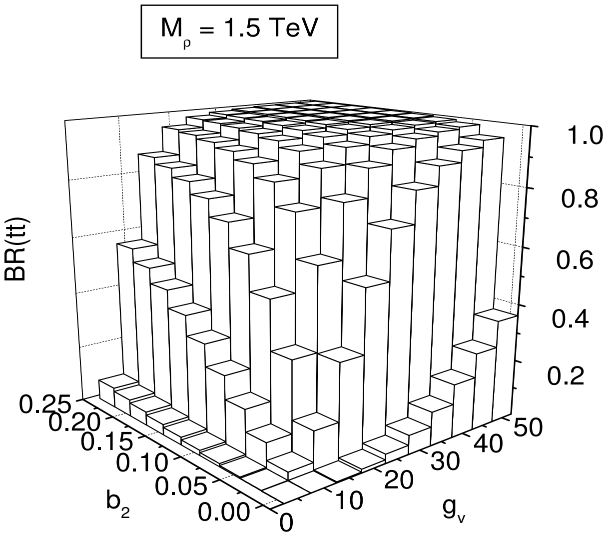

Fig.11a $\sigma(pp \to \rho t\bar{t})$

Fig.11b $BR(t\bar{t})$

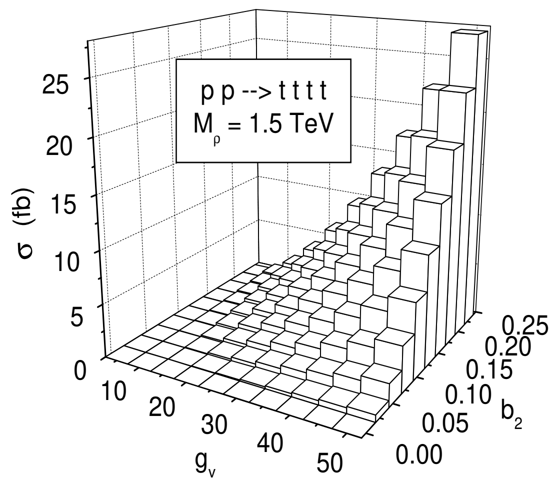

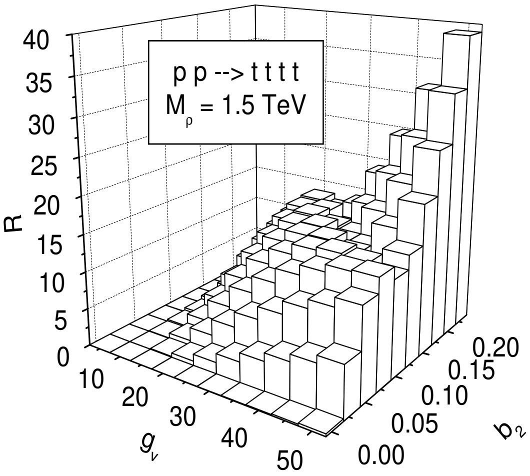

Fig.11c $\sigma = \sigma(pp \to \rho t\bar{t}) \times BR(t\bar{t})$

Fig.11d *Statistical significance R*